

# **Evaluating the Validity of 1D-CARS Using a Single Laser**

A Technical Report submitted to the Department of Mechanical and Aerospace Engineering

Presented to the Faculty of the School of Engineering and Applied Science  
University of Virginia • Charlottesville, Virginia

In Partial Fulfillment of the Requirements for the Degree  
Bachelor of Science, School of Engineering

**Miles Nicholas Coe**

Spring, 2020.

On my honor as a University Student, I have neither given nor received unauthorized aid on this assignment as defined by the Honor Guidelines for Thesis-Related Assignments

Chloe E. Dedic, Department of Mechanical and Aerospace Engineering

## Goal

The objective of this study was to evaluate the feasibility of 1-dimensional hybrid femtosecond/picosecond coherent anti-Stokes Raman scattering (1D fs/ps CARS) executed using a single femtosecond (fs) laser rather than using two separate laser systems (Bohlin, Patterson, & Kliewer, 2013).

## Background

Spectroscopy is the study of the interaction between light and matter (Graybeal, Hurst, Stoner, & Chu, 2018). Spectroscopy is used heavily in the fields of biology, chemistry, and physics to help gain insight into the processes and matter surrounding us. Advances in technology have allowed spectroscopy to be utilized to understand phenomena ranging from the micron scale up to the macroscale, such as the study of our solar system (NASA). Coherent Anti-Stokes Raman Spectroscopy (CARS) is a specific spectroscopy technique that provides excellent spatial and temporal resolution in the identification of chemical species and temperatures (Eckbreth, 1996). CARS was first developed in the 1970s and owes its existence to enhancements in high power nanosecond (ns) lasers, as well as compact picosecond (ps) and femtosecond (fs) lasers (Roy, Gord, & Patnaik, 2010). The CARS method uses three laser beams focused at a common point, commonly referred to as the pump beam, Stokes beam, and probe beam (Eckbreth, 1996). The frequencies of the pump and Stokes laser beams are chosen so that their difference matches the frequency of the target molecule (Roy, Gord, & Patnaik, 2010). The probe beam then scatters off the induced resonance and, through the conservation of momentum and energy, produces a fourth laser-like signal, referred to as the CARS signal. The generated signal is directed to a spectrometer where the spectral lines reveal information about the concentration and temperature of the target

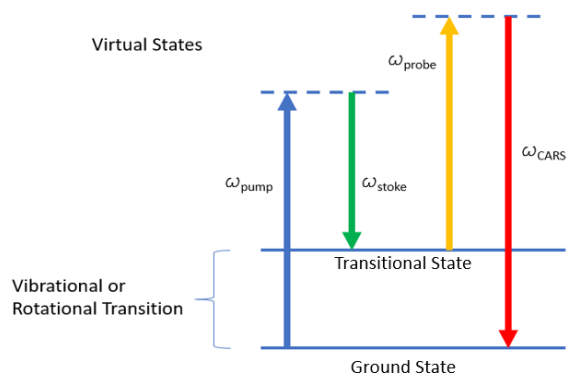


**Figure 1: Interaction of Pump, Stokes, and Probe Beam to Produce CARS Signal**

species (Equation 1) (Eckbreth, 1996). Since the CARS spectra produced is temperature dependent, it has become a particularly useful technique in the study of combustion and reacting flows (Oxford Instruments).

The CARS method has been applied to measure multiple species in reacting flows, measure species in flows that are typically difficult to study, high pressure environments, and in transient environments where high bandwidth and many measurements are necessary (Roy, Gord, & Patnaik, 2010). CARS can therefore provide insight into reacting flow environments that are conventionally difficult to measure. CARS allows for “in-situ” measurements that do not alter the chemistry or flow of the species being observed. Traditional temperature measurement techniques could involve inserting a thermocouple or other probe into the flow or taking a gas sample from the reactor, causing unwanted chemical reactions and perturbations to the flow; some flows can even be too hot and melt these thermocouples. Extensive research is being done using CARS to understand the process of soot formation and oxidation, which will be necessary to reduce these pollutants (Geigle, et al., 2005). CARS is also being used to help understand the complicated interactions that take place during combustion close to surfaces, interactions that are critical to the performance of internal combustion engines and gas turbines (Bohlin, Jainski, Patterson, Dreizler, & Kliewer, 2017). Increased efficiency and decreased pollution are possible if the fundamental mechanisms of combustion are better understood, studied using non-intrusive tools such as CARS.

Fs/ps CARS setups use an optical grating to disperse the fs laser pulse into its component wavelengths, then the desired wavelength is selected using a slit (Miller, 2012). This generates a frequency-narrow, ps duration laser pulse. Unwanted wavelengths terminate around the edges of the slit and the small subset of desired wavelengths travels through the slit and is reflected back

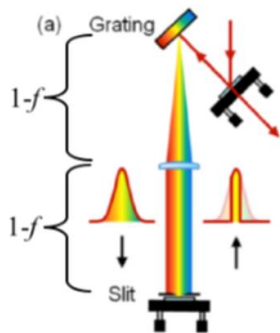


**Figure 2: Typical CARS Grating Setup**  
**Filtering out a Small Range of**  
**Wavelengths (Miller, 2012)**

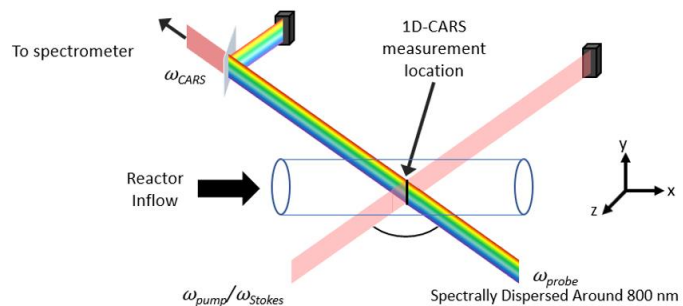


**Figure 3: 1D CARS Setup**

out of the pulse-shaper (Figure 2). Selecting a small range of wavelengths correlates to a temporal bandwidth as specified by the Time Bandwidth Product (TBP) (Equation 2). This phenomenon is a property of the Fourier transform between time and frequency space and defines how wide temporally or spectrally a pulse can be when it is approaching this transform limit.

By using a similar grating, but not filtering out wavelengths, the goal is to create a laser sheet where each position in space contains a small packet of spectral bandwidth. Each spectral unit will then be of the desired temporal bandwidth. Because more energy will be available, 1D measurements will be possible instead of needing to focus all of the probe energy to a single point. The pump and Stokes beams will be uniform in wavelength and dispersed and focused to a sheet by various lenses. The resulting CARS signal will be distributed over a line in space within the reacting sample, and the signal will be relay imaged into a spectrometer for detection.

Typically, a small range of wavelengths is desired in order to produce the CARS signal relevant to the species in question. By tuning the central wavelength of the laser, it may be possible to produce a measurable CARS signal along the entire line of intersecting pump, Stokes, and probe beams. Points along the line will be imaged by a spectrometer with a resolution of around 50 microns, yielding many points where valuable data can be collected at the same time. The temperature of each flame location will be determined by fitting spectral data with a Boltzmann distribution. Each peak in the intensity versus frequency shift graph (Figure 4) represents different electronic energy transitions. Based on the intensity of each transition and the overall distribution, the temperature of the reacting species can be determined. Equation 1 calculates the total intensity of electronic transitions between states  $i$  and  $f$  which makes up one peak of the entire Boltzmann distribution used for determining temperature (Figure 4) (Eckbreth, 1996).

$$\Delta\rho_{i \rightarrow f} = \frac{g_f}{\sum_m g_m \frac{-E_m}{k_B T}} \left[ e^{\frac{-E_i}{k_B T}} - e^{\frac{-E_f}{k_B T}} \right]$$

**Equation 1: Intensity of Electronic Transitions Between States  $i$  and  $f$  (Eckbreth, 1996)**

$$TBP = \Delta w \cdot \Delta t$$

**Equation 2: Time Bandwidth Product**

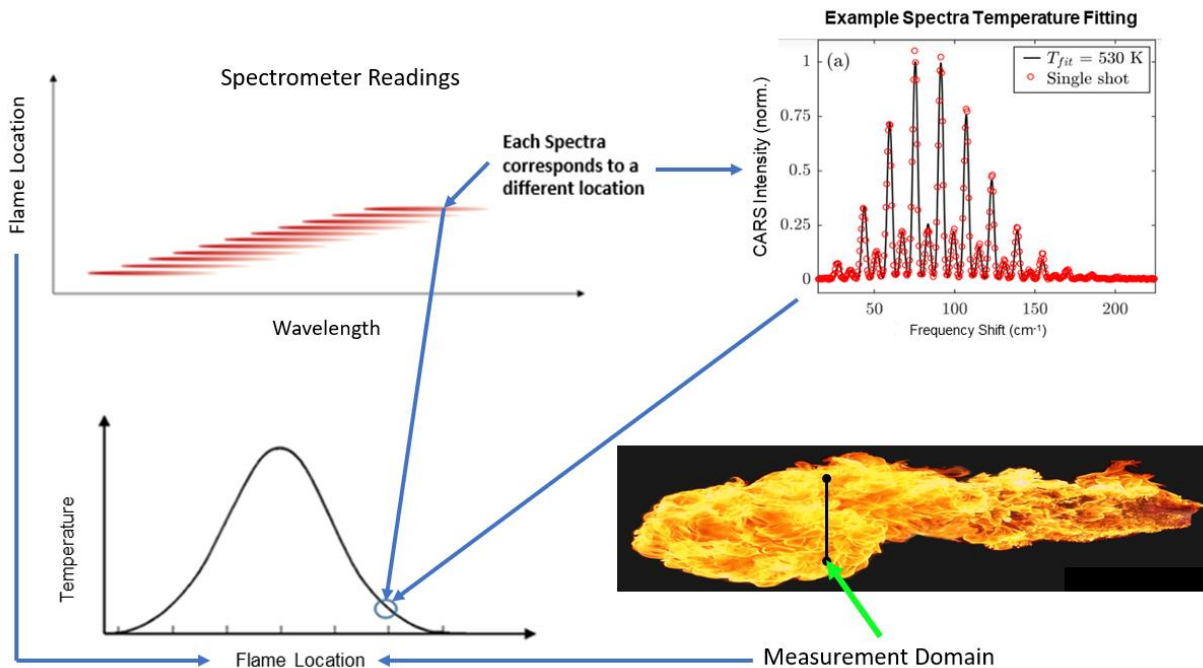


**Figure 4: Schematic Demonstrating how Temperature Profiles are Extracted from the Expected 1D CARS Data**

By investigating and validating a simplified line-CARS setup, researchers will be able to perform 1D fs/ps CARS with a single fs laser, instead of using separate fs and ps lasers synchronized in time. The recent development of 1D fs/ps CARS increases laser system complexity and cost dramatically compared to conventional point-CARS setups. Through this work, the point-CARS method which is more commonly applied can then be transformed into line-CARS without having to buy additional expensive lasers and other equipment.

### Objectives

In order to evaluate the feasibility of a 1D fs/ps CARS system, the subcomponents of the system must be evaluated. Importantly, the 60 fs, 18nm bandwidth beam (centered at 800 nm) available had to be characterized in order to be used as a 1D narrow-band probe “sheet.” Reimaging the generated signal would also have to be tested in order to support a full 1D system. Only then could a full 1D fs/ps CARS system be devised and tested.

## Theoretical Calculations

The first goal of initial calculations was to determine the characteristics of a dispersed beam after a holographic grating to determine if the dispersed beam could actually be used as a probe beam in a 1D-CARS setup. In order to do this, the dispersion equation was utilized. It takes the diffraction order and grating density of a specific grating and outputs the angle of dispersion based upon a given input angle of incident light.

Equation 3 and Figure 5 show how the diffraction equation can be utilized to determine the spatial dispersion of light after a dispersion grating. Different focal length convex lenses can be used in order to properly focus the light to a desired spatial dispersion.

In order to create many imageable points necessary for 1D-CARS, the grating would have to produce enough energy at 50-micron increments (spatial resolution of the system). Plots were generated in MATLAB in order to determine the theoretical duration, bandwidth, and intensity of light at each 50 micron imageable point (Figure 7).

Figure 7 shows how a laser pulse would vary in duration, bandwidth, and energy at a 50 micron imageable point within the laser beam. Based on typical 0D CARS setups, a ~5ps pulse with a bandwidth of ~3  $\text{cm}^{-1}$  is desirable. Based on the desired experimental parameters, a 1200 groove/mm holographic optical grating was the best choice. The energy per pixel was not low enough to deter the projected path of investigation. By using different focal length lenses when focusing the dispersed beam, pulse duration could be varied from about 2.5 to 7.5 ps and bandwidth from 2 to 5  $\text{cm}^{-1}$ .

## Experimental Setup

Once the theoretical calculations were complete, it was necessary to characterize the properties of the probe beam experimentally. The laser was routed from the conventional point-CARS optical setup to a small optical table where measurements with a fiber optic Ocean Optics

$$B_{+/-} = \sin^{-1}\left(\frac{m \cdot \lambda_{+/-}}{d} - \sin \alpha\right)$$

Equation 3: Grating Dispersion Equation

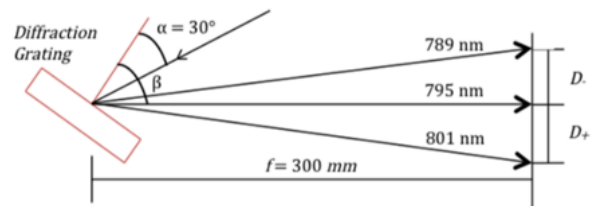
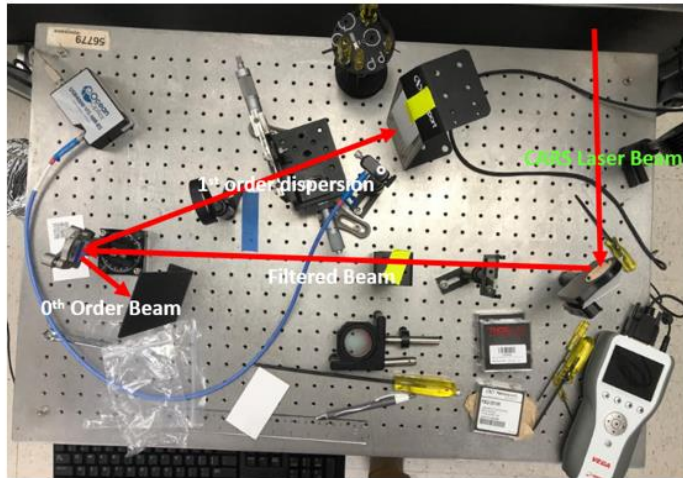


Figure 5: Holographic Grating Dispersion Schematic  
(Miller, 2012)



**Figure 6: Spectrometer Measurement Setup**

spectrometer (USB-4000-VIS-NIR-ES) were conducted. A 1200 groove/mm groove density grating had been purchased for these measurements.

The experimental setup is shown in Figure 6. The diverted beam enters the mini optical table from the top right and is then directed left to the 1200 groove/mm holographic optical grating. The 0<sup>th</sup> order beam terminates at a beam dump and the 1<sup>st</sup> order beam propagates through a horizontally adjustable vertical slit. The portion of the beam that travels through the slit terminates on a white business card so that the resulting spectrum can be measured.

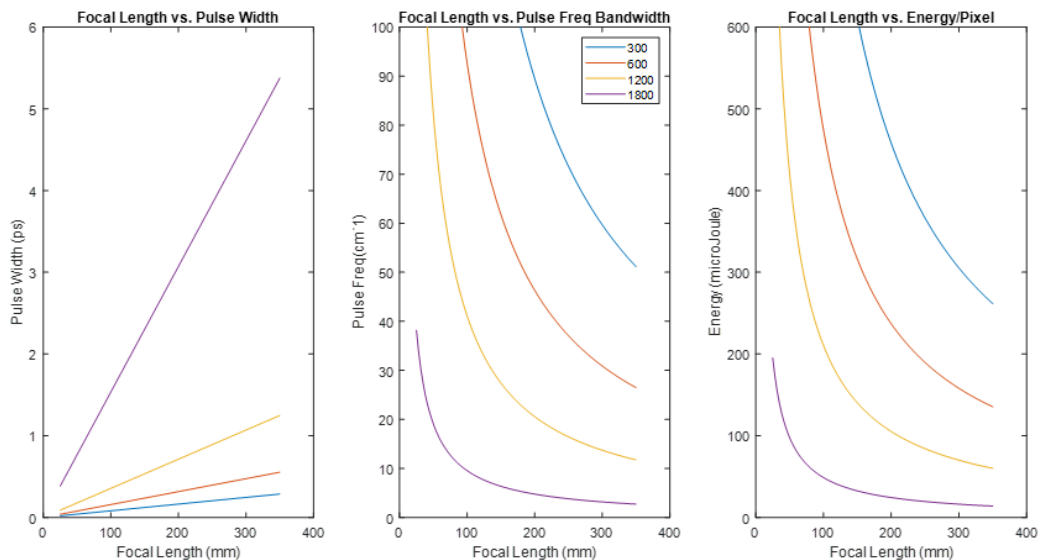


**Figure 7: Pulse Width, Bandwidth, and Energy for Different Focal Lengths and Gratings**

The Ocean Optics spectrometer has a fiber optic tip that can be angled directly at the business card in order to collect this data. A laser power meter was also used to ensure that the chosen input angle to the grating produced an optimal efficiency. About 10 microjoules is necessary at each imageable point in order to produce a measurable 1D-CARS signal. Since the energy of the spatially filtered beam is great enough to saturate the Ocean Optics spectrometer, a filter was used to lower the energy of the beam. It was also preferable to use a filter to prevent the high laser energy from damaging the holographic grating. Using the power meter, the unfiltered energy of the laser beam was about 3.52 W. The filtered beam was measured to be 482 mW, meaning the filter allowed about 7.3% of the laser energy to pass. The grating angle was then optimized to give 349 mW of power of the first order beam. This represents a 72.4% efficiency of the grating which is similar to the specified maximum efficiency of the grating.

Next, a slit width of .014" was chosen so that the energy of the beam was able to be detected by the Ocean View Spectrometer. This .014" slit was traversed perpendicularly along the dispersed beam after the grating and one focal length (the image plane) away from the 150mm focal length lens. Because this was larger than the actual spatial width of interest, 50 microns (.002"), the slit width used in these measurements was too large to provide data directly comparable to energy a spectrometer camera pixel would receive. The .014" slit was a limitation of the mechanical slit as well as sensitivity of the fiber optic spectrometer. Calculations were conducted again with a .014" imageable point resulting in a theoretical pulse duration of .534 ps,

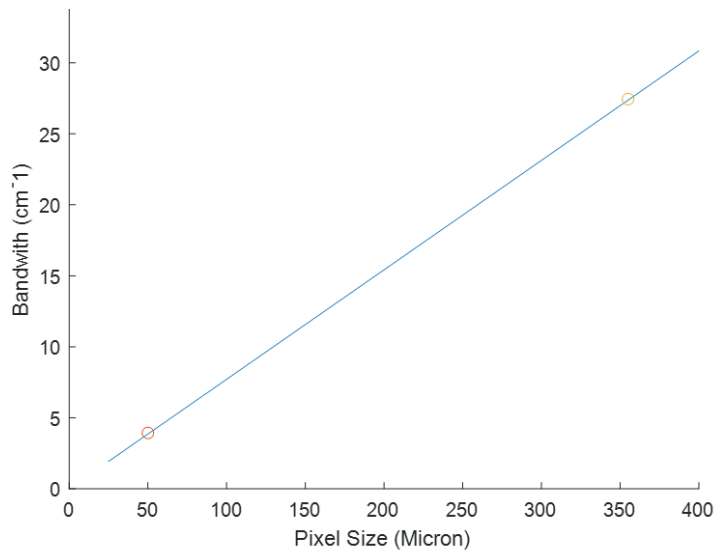


**Figure 8: Bandwidth vs. Pixel Size**

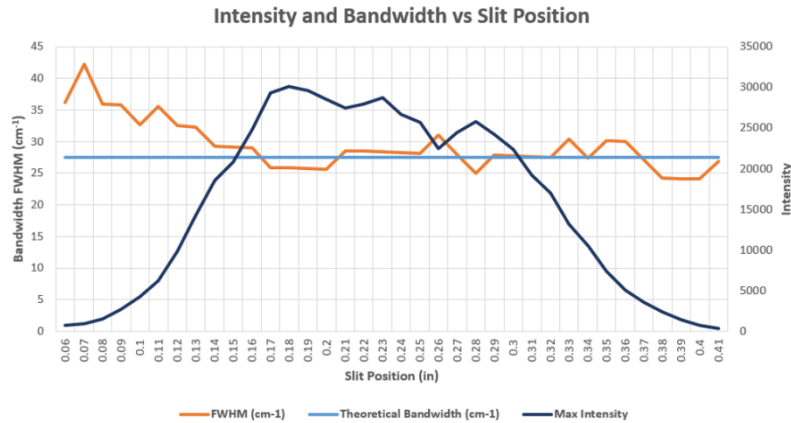


**Figure 9: Adjusted Bandwidth and Intensity vs. Slit Position**

bandwidth of  $27.5 \text{ cm}^{-1}$ , and energy of  $140.5 \mu\text{J}$ . Figure 8 shows how bandwidth varies based on the size of the slit used. The 50 micron and 355 micron points correspond to the .002” and .014” slits respectively. Figure 10 shows the experimental Gaussian distributions obtained at each slit position.

Figure 9 shows the relative intensity of spectrometer readings as well as the bandwidth (in  $\text{cm}^{-1}$ ) compared to the theoretical  $27.5 \text{ cm}^{-1}$  bandwidth for a 150mm focal length lens with a 1200 groove/mm grating. Spectrometers do not have perfect resolution, meaning that if an infinitely narrow bandwidth beam was read into the spectrometer then the spectrometer would register a finite bandwidth—defined as the instrument function of the spectrometer. In order to estimate the

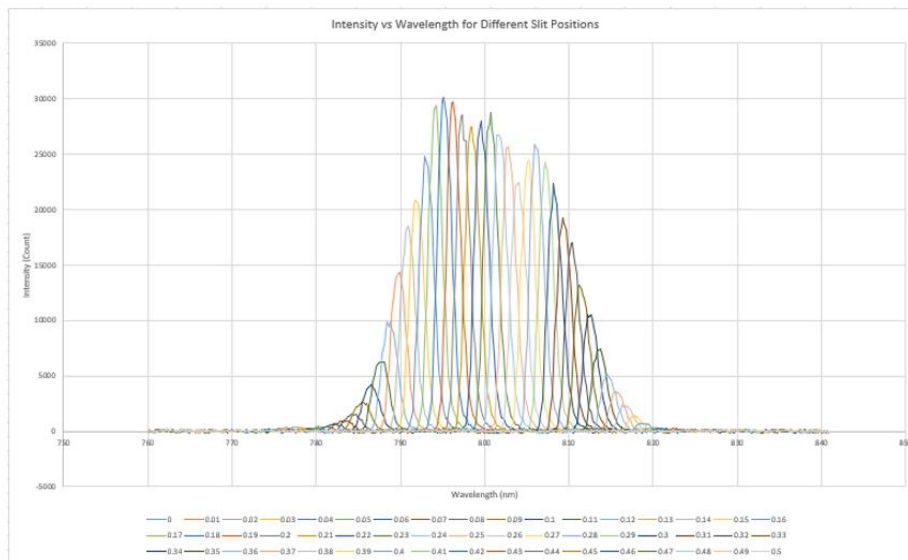


**Figure 10: Slit Position vs. Wavelength Raw Data**

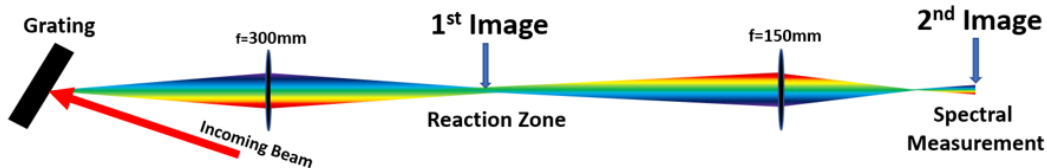


Figure 11: 2f Re-Imaging Schematic

instrument function of the fiber optic spectrometer used, it was assumed that an infinitely narrow bandwidth beam would register across 6 pixels of the spectrometer. The ranges register wavelengths at a resolution of about .186 nm so this simplification assumes that the instrument function would be 1.12 nm. A simulated Gaussian, centered at 800 nm, was created to model this and it was determined that the FWHM was 0.25 nm when a Gaussian was dispersed across 6 pixels. The measured bandwidth of the spectrometer is a function of the convolution of the instrument function of the spectrometer and the actual bandwidth of the beam. FWHM values can be converted into variances of the gaussians, and by subtracting the instrument function variance from the measurement variance, the actual measurement variance can be determined. Using this relationship, each spectrometer measurement can be corrected to more accurately characterize the measured bandwidths. Figure 9 shows the adjusted measured bandwidths compared to the theoretical bandwidth of  $27.5 \text{ cm}^{-1}$ , and there is good agreement between the measured bandwidth and the bandwidth originally calculated.

Measurements confirmed the theoretical bandwidth of  $27.5 \text{ cm}^{-1}$  and the intensity of the beam at different positions varied in an expected manner. The next step was to complete similar measurements by reimaging the probe beam with a spectrometer capable of performing full 1D CARS.

Reimaging is necessary in a CARS setup since the reaction being analyzed must occur at the first image plane and information collected by a spectrometer must occur at the second image plane. A higher-powered spectrometer would further characterize the grating-disperse probe beam. A 2f (2 focal length) imaging system was devised to qualitatively observe reimaging when a grating is involved. Figure 11 is the optical diagram for forming the ps laser sheet (1st image) and reimaging the generated CARS beam at the entrance to a spectrometer (2nd image). The first lens (300 mm) is used to image the spectral dispersion in one dimension and focus the light in the other.

By visual inspection, relay imaging was successful. Crisp edges and identical spectral variations were observed in the second image plane.

### Future Work

Imaging with a high-powered spectrometer is necessary to fully characterize the dispersed probe beam and ensure the energy and intensity of the laser pulse at different locations is sufficient to produce a CARS signal. Once these measurements are conducted, work can begin on constructing a full 1D fs/ps CARS system. In typical 0D CARS systems, the probe beam can be filtered leaving only the CARS signal to be measured by a spectrometer. Due to the probe beam containing a relatively large range of bandwidths overlapping with bandwidths generated in the CARS signal, filtering is not an option. The conservation of momentum principle of light must then be used to direct the CARS signal separately from the probe beam. If the probe, Stokes, and pump beams interact at different angles, then the CARS signal will propagate separately, allowing independent measurement.

Timing is essential in any CARS setup. All three beams must overlap at the measurement volume at the same time within 60 fs, requiring identical path lengths within 18  $\mu\text{m}$ . The pump and Stokes beam must arrive at the measurement plane at the same time, whereas the probe beam

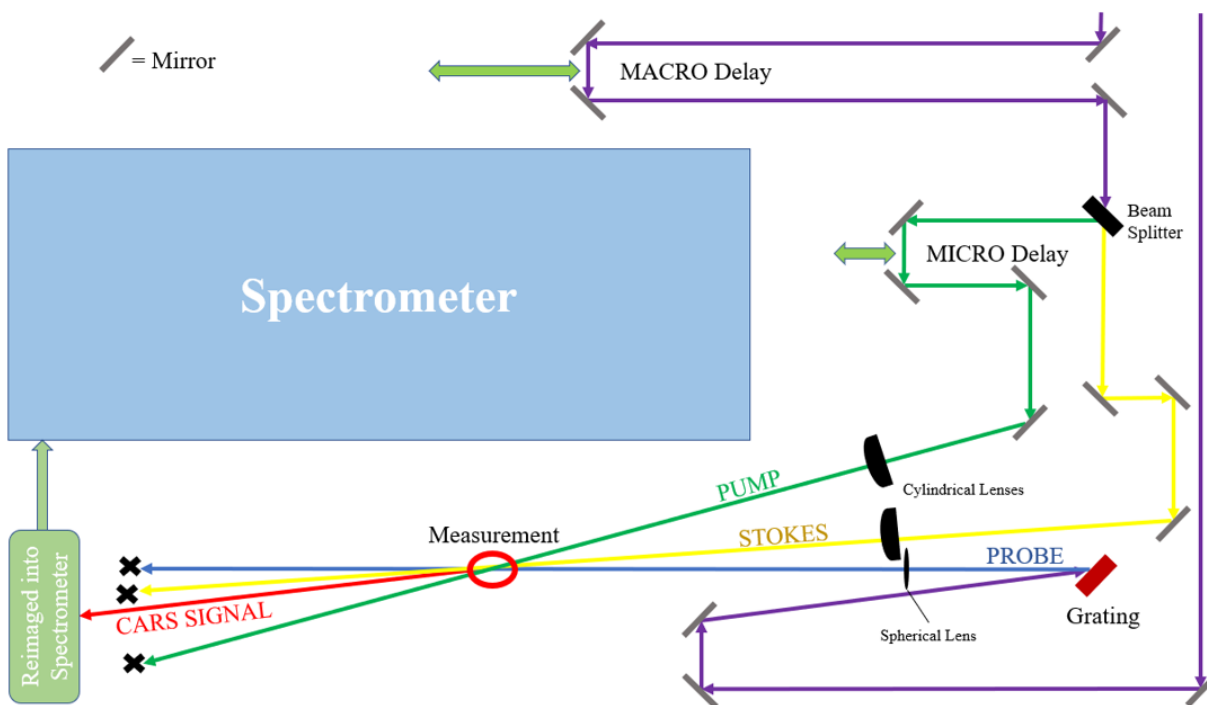


Figure 12: Preliminary 1D CARS Optical Setup

arrives later on the order of ps. In order to achieve precise timing, optical delay stages are used. A large stage will be used to time the delayed probe pulse, and a small stage can be used to temporally align the pump and Stokes pulse. Figure 12 shows the optical diagram for future single-laser 1D fs/ps CARS measurements. The proposed setup allows all 3 beams to traverse 45 inches and therefore reach the measurement plane at the same time. The stages allow for small adjustments, and varying the placement of the stages (denoted by the double arrows in Figure 12) will allow overall timing to be adjusted accurately. Each of the lenses shown will be placed exactly one focal length away from the measurement plane.

### **Conclusion**

The calculations and measurements conducted thus far support the plausibility of a 1D fs/ps CARS system utilizing a single laser source. Further work is necessary to fully prove the utility and resolution of such a system. The noninvasive nature of the measurement and excellent spatial and temporal resolution has made CARS the gold-standard of quantitative combustion spectroscopy. Extending the conventional single-point measurement to a 1-dimensional line has allowed for the resolution of spatial gradients within a reacting system, but is so far limited to expensive, two-laser systems. However, this study has demonstrated the feasibility of using a single laser to perform 1D fs/ps CARS measurements, enabling a 1-dimensional CARS system that is more affordable and accessible for future researchers.

## Sources

- Bohlin, A., Jaini, C., Patterson, B. D., Dreizler, A., & Kliewer, C. J. (2017). Multiparameter spatio-thermochemical probing of flame–wall interactions advanced with coherent Raman imaging. *Proceedings of the Combustion Institute*, 36(3), 4557–4564. doi: 10.1016/j.proci.2016.07.062
- Bohlin, A., Patterson, B. D., & Kliewer, C. J. (2013). Communication: Simplified two-beam rotational CARS signal generation demonstrated in 1D. *The Journal of Chemical Physics*, 138(8), 081102. doi: 10.1063/1.4793556
- Eckbreth, A. C. (1996). *Laser diagnostics for combustion temperature and species*. Amsterdam: Gordon & Breach.
- Geigle, K. P., Schneider-Kühnle, Y., Tsurikov, M. S., Hadeif, R., Lückerrath, R., Krüger, V., ... Aigner, M. (2005). Investigation of laminar pressurized flames for soot model validation using SV-CARS and LII. *Proceedings of the Combustion Institute*, 30(1), 1645–1653. doi: 10.1016/j.proci.2004.08.158
- Graybeal, J. D., Hurst, G. S., Stoner, J. O., & Chu, S. (2018, June 8). Spectroscopy. Retrieved from <https://www.britannica.com/science/spectroscopy>.
- Miller, J. D. (2012). Hybrid femtosecond/picosecond coherent anti-Stokes Raman scattering for gas-phase temperature measurements. doi: 10.31274/etd-180810-2935
- NASA. (n.d.). Spectroscopy. Retrieved from <https://scienceandtechnology.jpl.nasa.gov/research/research-topics-list/spacecraft-technologies/spectrometry>.

Oxford Instruments. (n.d.). Combustion Spectroscopy - Coherent anti-Stokes Raman Spectroscopy - Andor Learning Centre. Retrieved from <https://andor.oxinst.com/learning/view/article/combustion-spectroscopy-coherent-anti-stokes-raman-spectroscopy>.

Roy, S., Gord, J. R., & Patnaik, A. K. (2010). Recent advances in coherent anti-Stokes Raman scattering spectroscopy: Fundamental developments and applications in reacting flows. *Progress in Energy and Combustion Science*, 36(2), 280–306. doi: 10.1016/j.pecs.2009.11.001